Laminar differences in gamma and alpha coherence in the ventral stream

Elizabeth A. Buffalo[a,1], Pascal Fries[b], Rogier Landman[c], Timothy J. Buschman[c], and Robert Desimone[c]

[a]Yerkes National Primate Research Center and Department of Neurology, Emory University School of Medicine, Atlanta, GA 30329; [b]Ernst Strüngmann Institute (ESI) in Cooperation with Max Planck Society, 60528 Frankfurt, Germany; and [c]McGovern Institute for Brain Research, Massachusetts Institute of Technology, Cambridge, MA 02139

Edited* by N. Kopell, Boston University, Boston, MA, and approved May 25, 2011 (received for review July 30, 2010)

Attention to a stimulus enhances both neuronal responses and gamma frequency synchrony in visual area V4, both of which should increase the impact of attended information on downstream neurons. To determine whether gamma synchrony is common throughout the ventral stream, we recorded from neurons in the superficial and deep layers of V1, V2, and V4 in two rhesus monkeys. We found an unexpected striking difference in gamma synchrony in the superficial vs. deep layers. In all three areas, spike-field coherence in the gamma (40–60 Hz) frequency range was largely confined to the superficial layers, whereas the deep layers showed maximal coherence at low frequencies (6–16 Hz), which included the alpha range. In the superficial layers of V2 and V4, gamma synchrony was enhanced by attention, whereas in the deep layers, alpha synchrony was reduced by attention. Unlike these major differences in synchrony, attentional effects on firing rates and noise correlation did not differ substantially between the superficial and deep layers. The results suggest that synchrony plays very different roles in feedback and feedforward projections.

electrophysiology | macaque | oscillation

Anatomical and physiological studies have characterized the afferent inputs to and efferent inputs from neurons in different layers of visual cortical areas. However, physiological distinctions across layers, such as synchronous interactions, have not been fully identified. We first came across laminar differences in synchrony serendipitously. Gamma-band synchrony, measured either by spike-field or spike-spike interactions across multiple electrodes, is a prominent feature in visual cortex, and several studies have shown that attention enhances gamma-band synchrony in area V4 (1–5). In our first recordings in area V1, we also found prominent gamma-band synchrony, although the effects of attention, if any, were much smaller than what we previously found in V4 (1). However, in our first recordings in area V2 in the lunate sulcus, we were surprised to find hardly any gamma-band synchrony. We initially had no explanation for why V2 should be so different from V1 and V4. Probing at greater electrode depths led to the discovery that V2 cells do show gamma-band synchrony but only at those deeper electrode depths. Because V2 in the lunate sulcus bends under V1, layer 6 cells are closer to V1 on the occipital surface than are layer 1 cells. Thus, our deeper electrode recordings were actually located in the more superficial layers of V2. Because we typically studied the first responsive cells found in any penetration, this must have strongly biased our first recordings in V2 to the deep layers, and these deep layers apparently had little gamma-band synchrony. Conversely, the same tendency to sample the first responsive cells on a penetration would have resulted in a strong bias to record cells in the superficial layers of V1 and V4, from which we recorded directly on the cortical surface. This possibility led us to test whether the deep layers of V1 and V4 were also lacking in gamma-band synchrony, as in V2.

In addition, we examined whether there are any laminar differences in attentional effects on synchrony, because the different layers play very different roles in sending information to other areas and have different cortical and subcortical projections. Several lines of research have shown that directed attention to a cued location leads to improved processing of visual stimuli at that location and attenuated processing of competing stimuli presented elsewhere (6). In visual cortex, attention enhances neuronal firing rates (7–11), reduces variance [e.g., decreased Fano factor and noise correlation (12–14)], and enhances gamma frequency synchrony (1, 3), all of which are thought to increase the signal to noise for attended signals and to increase their impact on neurons in downstream areas (15–17). There is also recent progress in understanding the nature of some of the attentional feedback to visual cortex from the frontal eye fields and parietal cortex (18), which appears to enhance firing rates and synchronize activity in the gamma range in visual cortex, at least in V4 and/or middle temporal area (MT) (19–21). However, any laminar differences in the effects of attention in visual cortex remain unknown.

Results

We recorded from a total of 226 small clusters of cells (multiunits, termed cells for convenience) and local field potentials (LFPs) on four to eight nearby electrodes in each recording session. Total cells recorded in the superficial layers of V1, V2, and V4 were 67, 13, and 73, respectively, and the corresponding totals in the deep layers were 14, 47, and 12. The superficial V4 cells included 47 cells reported in previous studies of coherence and attention in V4 (1), and individual cells from recordings in all three areas were included in a previous study of attentional effects on firing rate latencies (22). Cells were recorded in two monkeys performing a task of directed spatial attention (Fig. 1*A*).

Coherence Differences Across Layers. The most striking differences in neuronal response measures in superficial vs. deep layers were in spike-field coherence (SFC). Fig. 1 shows the SFC spectra for attend-in and attend-out conditions averaged from the population of recordings in all three areas. For each spike-field pair, the spike and LFP signals were taken from separate electrodes recorded simultaneously and located in the same layer (superficial or deep). Independent of attention, the superficial layers of all three areas showed a strong peak in gamma, from about 40–60 Hz (Fig. 1 *B–D*).

By contrast, the SFC in the deep layers was almost the mirror image of the pattern in the superficial layers (Fig. 1 *E–G*). Coherence in gamma was minimal; there was only a slight bump in gamma in the deep layers in V1 and V4 and no gamma bump at all in V2. Moving into the lower frequencies, coherence rose sharply beginning at about 35 Hz. Coherence peaked at about 10 Hz, in the alpha range, in V1 and V2. For convenience, we

Author contributions: E.A.B., P.F., and R.D. designed research; E.A.B., P.F., R.L., and T.J.B. performed research; E.A.B. analyzed data; and E.A.B. and R.D. wrote the paper.

The authors declare no conflict of interest.

*This Direct Submission article had a prearranged editor.

[1]To whom correspondence should be addressed. E-mail: elizabeth.buffalo@emory.edu.

This article contains supporting information online at www.pnas.org/lookup/suppl/doi:10.1073/pnas.1011284108/-/DCSupplemental.

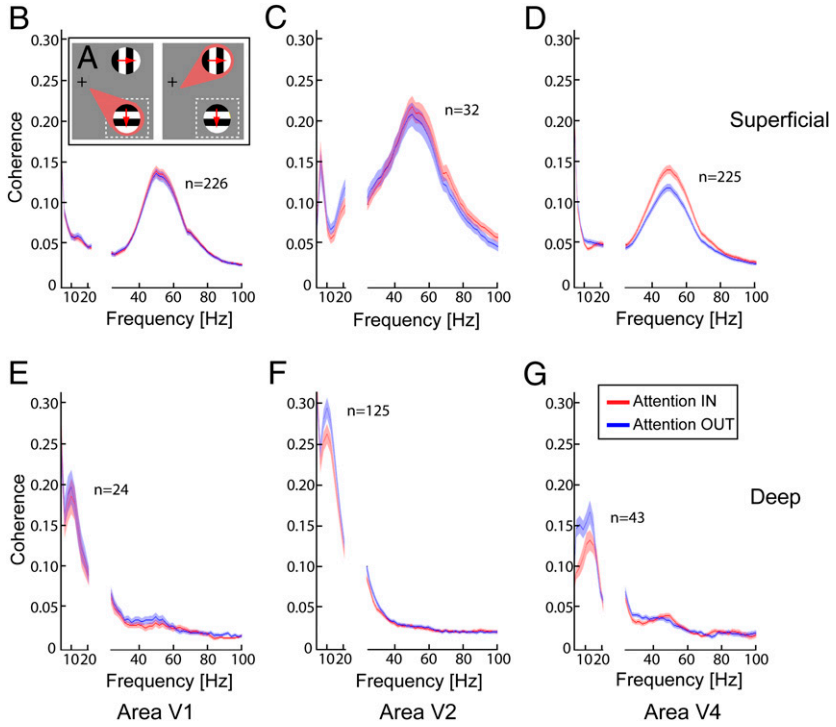

Fig. 1. Attentional modulation of SFC in areas V1, V2, and V4. (*A*) On alternating blocks of trials, monkeys were cued to attend to a moving grating either inside (top) or outside (bottom) of the recorded neuron's RF. Red traces represent SFC in each area, with attention directed INTO the neuron's RF. Blue traces represent SFC with attention directed OUT of the RF. The magnitude of coherence as a function of frequency is shown for superficial recordings (*B–D*) and deep recordings (*E–G*) for areas V1 (*B* and *E*), V2 (*C* and *E*), and V4 (*E* and *G*). Shaded areas represent SEM.

will refer to the observed 6- to 16-Hz band as "alpha," although it extends from high theta, through alpha, to low beta. Coherence below 4 Hz, not shown in Fig. 1, was often phase-locked to the drifting grating frequency, and it was slightly enhanced by attention in V4. In the superficial layers of all three areas, SFC rose steadily in moving down from 20 to 4 Hz, but there was no peak in alpha (there was even a suggestion of a trough in alpha) and the magnitude of coherence in alpha did not reach the magnitude of coherence at gamma. The differences between the superficial and deep layers in gamma-band vs. alpha-band SFC can also be seen in Fig. 2*A*, which shows the distribution of gamma- and alpha-band SFC in the superficial and deep cortical layers for all recording sites in area V4. Fig. S1 shows the results for areas V1 and V2. In some layers and areas, we obtained data primarily from one or the other monkey; however, a similar pattern of effects was observed across layers and areas (Fig. S2).

A further distinction between layers was revealed in the effect of visual stimulation on alpha-band coherence (Fig. S3). For the superficial layers, there was a significant decrease in alpha on stimulus onset (compared with the prestimulus baseline) for all

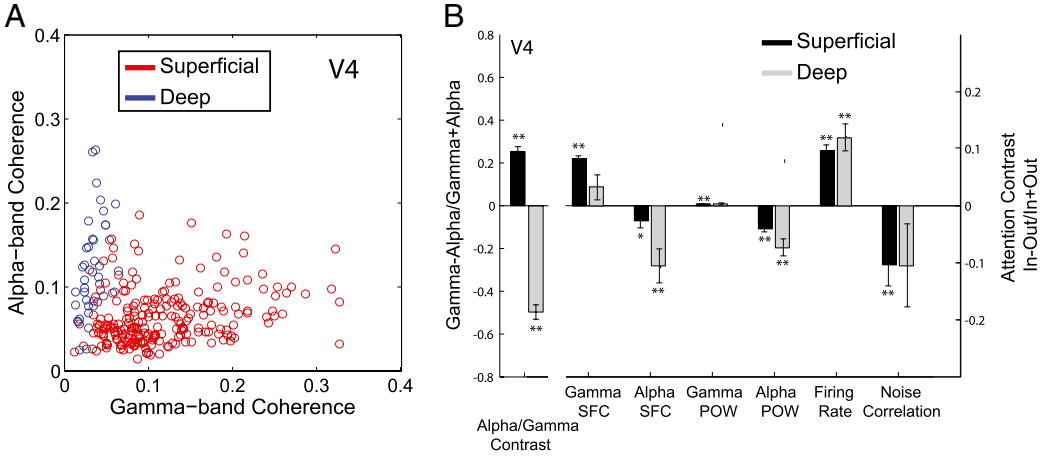

Fig. 2. Laminar effects in area V4. (*A*) Distribution of coherence in gamma- and alpha-bands for superficial and deep recordings in area V4. Superficial layer recordings (red) demonstrated stronger gamma-band coherence, whereas deep layer recordings (blue) demonstrated stronger alpha-band coherence. (*B*) Attentional effects across superficial and deep layer recordings in area V4. Contrast indices (In − Out/In + Out) of the effects of attention were calculated for several measures. Superficial recordings are shown in black, and deep recordings are shown in gray. **P* < 0.05; ***P* < 0.01. All comparisons are sign tests, relative to zero.

three areas [V1: $t(225) = 5.97$, $P < 0.001$; V2: $t(31) = 3.52$, $P < 0.01$; V4: $t(224) = 15.54$, $P < 0.001$], consistent with previous reports (3). By contrast, the deep layers of areas V1 and V2 showed a significant increase in alpha-band SFC at stimulus onset [V1: $t(23) = -3.29$, $P < 0.01$; V2: $t(124) = -23.09$, $P < 0.001$]. In the deep layers of V4, there was a small decrease in alpha after stimulus onset, which reached statistical significance [$t(42) = 2.16$, $P < 0.05$].

Attention Effects on Coherence Across Layers. The difference in gamma- vs. alpha-band SFC between layers was paralleled by differences in the effects of attention on coherence. Whereas gamma-band coherence in the superficial layers was enhanced with attention, alpha-band coherence in the deep layers was suppressed with attention. To examine the distribution of these effects across all spike-field pairs, we calculated a contrast index of attentional effects for each pair in both the alpha- and gamma-frequency bands (Fig. 2*B* and Fig. S4). The attention index was computed according to the following formula within each frequency band: attend IN − attend OUT/attend IN + attend OUT for all spike-field pairs. Across the population of superficial recordings in each visual area, gamma-band (40–90 Hz) SFC was increased with attention. In V1, gamma-band SFC was increased by a median of 2% with attention, although it did not reach significance (131 increases, 95 decreases; paired sign test, $P = 0.06$). When we analyzed the V1 attentional effect in each monkey separately, there was a significant effect of attention on gamma-band SFC in monkey M1 (79 increases, 47 decreases; paired sign test, $P < 0.01$) but not in monkey M2 (52 increases, 48 decreases; paired sign test, $P > 0.1$). In V2, gamma-band SFC was increased by a median of 4% with attention (26 increases, 6 decreases; paired sign test, $P < 0.001$), and in V4, gamma-band SFC was increased by a median of 8% with attention (198 increases, 27 decreases; paired sign test, $P < 0.001$). By contrast, there was no significant effect of attention on gamma coherence in the deep layers of any of the three areas ($P > 0.05$ for all values).

In contrast to the enhancement of gamma by attention in the superficial layers, attention reduced alpha coherence in the deep layers. Across the population of deep recordings in areas V2 and V4, alpha (6–16 Hz) SFC was significantly decreased with attention. In V2, alpha-band SFC was decreased by a median of 5% with attention (28 increases, 97 decreases; paired sign test, $P < 0.001$), and in V4, alpha-band SFC was decreased by a median of 10% with attention (9 increases, 34 decreases; paired sign test, $P < 0.001$). In the deep layers of V1, alpha SFC was decreased by a median of 3% with attention, but this decrease failed to reach significance (9 increases, 15 decreases; paired sign test, $P > 0.10$). Among the superficial layers, there was a significant decrease in alpha coherence with attention only in area V4 (median = 4% decrease; 89 increases, 136 decreases; paired sign test, $P < 0.05$).

We also examined spike-spike coherence (SSC) in the superficial and deep layers of all three areas, and the results, shown in Fig. S5, paralleled the results from analyzing SFC. Specifically, the superficial layers showed a large gamma peak in SSC, which was significantly enhanced by attention in V2 and V4 (V2: 7 increases, 2 decreases, paired sign test, $P < 0.05$; V4: 67 increases, 33 decreases, paired sign test, $P < 0.001$), whereas the deep layers showed a large low-frequency peak in alpha frequencies, which was significantly desynchronized by attention in all three areas (V1: 1 increase, 11 decreases, paired sign test, $P < 0.001$; V2: 10 increases, 33 decreases, paired sign test, $P < 0.001$; V4: 4 increases, 13 decreases, paired sign test, $P < 0.01$).

Other Effects of Attention Across Layers. In contrast to the consistent differences in SFC and SSC between superficial and deep layers, there were smaller and less consistent differences in LFP power in the superficial and deep layers. As shown in Fig. 2*B* and Fig. S4, in the superficial layers of V2 and V4, there was a small but significant increase in gamma power with attention (V2: 9 increases, 4 decreases, paired sign test, $P < 0.05$; V4: 51 increases, 22 decreases, paired sign test, $P < 0.001$). There were no differences across attention conditions in the gamma power of the deep layers ($P > 0.05$ for all values). By contrast, there was a decrease in alpha power with attention in the deep layers of areas V1, V2, and V4 (V1: 3 increases, 11 decreases, paired sign test, $P < 0.05$; V2: 11 increases, 36 decreases, paired sign test, $P < 0.001$; V4: 1 increase, 11 decreases, paired sign test, $P < 0.001$), as well as in the superficial layers of V2 and V4 (V2: 1 increase, 12 decreases, paired sign test, $P < 0.001$; V4: 9 increases, 64 decreases, paired sign test, $P < 0.001$).

The difference in attentional effects on coherence in the superficial and deep layers raised the question of whether there were other differences in the effects of attention across layers. Fig. 2*B* and Fig. S4 compare the alpha/gamma contrast index found in the superficial and deep layers with comparable contrast indices for attentional effects on alpha and gamma coherence, LFP power, firing rates, and the cross-trial "noise correlation." As described above, there was a very large difference in gamma and alpha coherence between layers. By contrast, attentional effects on firing rates were not significantly different across layers, but there was a significant effect of area, with the largest effects in area V4 (two-way ANOVA, main effect of area [$F(2,222) = 9.89$, $P < 0.001$; main effect of layer [$F(1,222) = 0.10$, $P > 0.05$]. Noise correlation refers to the correlation in firing rates recorded across pairs of electrodes measured over trials, and two recent studies have shown that noise correlation is significantly reduced with attention in area V4 (13, 14). We calculated the Pearson correlation for all pairs in all layers; as shown in Fig. 2*B* and Fig. S4, there was no significant difference in noise correlations across layers. However, although the largest effects were in area V4, a two-way ANOVA revealed no significant main effects of area or layer [main effect of area $F(2,235) = 1.07$, $P > 0.05$; main effect of layer $F(1,235) = 0.04$, $P > 0.05$]. Thus, despite the large difference in SFC and SSC between superficial and deep layers, attentional effects on firing rates and noise correlation seemed comparable across layers.

Discussion

The laminar differences in synchrony described here are roughly consistent with a laminar model of attention proposed by Grossberg (23). Although prior studies have not localized gamma- and alpha-band coherence to the superficial and deep layers under the conditions we have studied here, data from slice recordings and anesthetized rat recordings have long suggested that alpha synchrony derives from pyramidal cells in layer 5 (24–26). Data from translaminar recordings in the visual cortex of dogs suggested that layer V cells are the cortical origin of the alpha rhythm, based on a phase reversal in this rhythm at about 1,100 μm below the cortical surface (27). A recent study in awake monkeys using translaminar electrodes also localized alpha synchrony primarily to the granular and infragranular layers in areas V2 and V4 (28). It is thought that these layer 5 pyramidal cells have two inward currents, known as the h and T currents, which have time constants consistent with alpha. Modeling studies have shown that such a cell, when coupled with a fast-spiking inhibitory neuron, will exhibit sustained alpha oscillations (29), although recent whole-cell recordings suggest that the alpha frequency oscillations of layer 5 cells derive mainly from excitatory inputs (26). Certain thalamic cells also exhibit alpha-band synchrony, and a thalamocortical anatomical loop may also play a role in generating cortical alpha (30).

The localization of gamma-band synchrony to predominantly the superficial layers has not previously been established in vivo, but it should be noted that kainate applied to layer 2/3 or layer 5

slices induces gamma-band oscillations only in cells in superficial layer slices, whereas low Mg (which stimulates NMDA receptors) induces alpha-band oscillations only in cells in layer 5 slices (25). A study of rat somatosensory cortex slices showed that kainate induced gamma oscillations in the superficial layers, beta2 oscillations in the deep layers, and mixed frequencies in layer 4 (31). The cat visual cortex also contains a class of pyramidal and stellate cells termed "chattering cells," which are localized to layers 2/3 and fire with high-frequency bursts in the gamma-frequency range (32, 33). A recent study in awake monkeys using translaminar electrodes also reported a predominance of gamma activity in the LFP of superficial layers in area V1 (34).

The superficial and deep layers not only had different peak coherence frequencies, but these peaks showed opposite effects of attention. Gamma coherence was enhanced by attention, whereas alpha coherence was reduced with attention, and both of these effects have been reported in prior attentional studies in area V4 (1, 3, 21). The enhancement of gamma synchrony with attention has been proposed to increase the impact of attended signals on downstream neurons in visual cortex as a result of the finite synaptic integration time of cortical neurons (1). Indeed, attention appears to enhance gamma synchrony across cortical areas (20, 21), at least for monosynaptically connected cortical areas (35). A desynchronization of alpha synchrony recorded with electroencephalography has long been associated with attention (36–39), and increased alpha power in the EEG or magnetoencephalogram predicts errors in perception tasks (40–42) and has been suggested to reflect an active attentional suppression mechanism (43–45).

We did not find the same desynchronization of coherence with attention at frequencies below 4 Hz. In fact, there was a small enhancing effect of attention on these low frequencies in V4. By contrast, a recent study reported strong desynchronization of frequencies below 5 Hz with attention in V4 (14). The most likely explanation for this difference is that our stimuli were gratings with a drift rate of 1–2 Hz, and there was a strong increase in intertrial coherence at low frequencies that began at stimulus onset. Thus, the temporal structure of our stimulus may have prevented any desynchronization of low-frequency coherence with attention. This explanation would also be consistent with recent results showing a strong increase in low-frequency coherence with attention in V1, in a cross-modal attention task with low-frequency alternation between visual and auditory stimuli (46). Schroeder and Lakatos (47) have proposed that in tasks with temporal structure to the stimuli, the attentional feedback will be frequency-modulated to enhance whatever frequency components are behaviorally useful.

Two recent studies have reported that attention decreases the noise correlation between simultaneously recorded neurons in area V4 (13, 14). If these correlations were attributable to coupled oscillatory fluctuations in activity, they would represent low-frequency (<5 Hz) coherence. Although the low-frequency desynchronization with attention found in one study (14) appeared to be strongly related to the decrease in noise correlation that was found, these two phenomena were dissociated in the present study in that we found that low-frequency synchrony in superficial V4 increased slightly with attention, whereas the noise correlation decreased with attention. Again, this difference is likely related to the low-frequency drift of the stimulus in our study, which caused cells to fire in a phase-locked fashion to the stimulus at these frequencies. Across areas, we found that attentional effects on noise correlation roughly paralleled the order of attentional effects on firing rates and gamma synchrony, in that the effect was strongest in V4 and nonsignificant in V1 and V2 (Fig. 2*B* and Fig. S4). The absence of an attentional effect on noise correlations in V1 was also reported previously (48).

We found a "backward" progression of attentional effects on synchrony in the ventral stream, with the strongest enhancement of synchrony in V4 and the weakest effects in V1, suggesting that V4 might be responsible for the attentional effects in upstream areas through feedback projections (22). Another recent study found an enhancement of gamma synchrony with attention in V4 but a suppression of gamma synchrony in V1 (49). That study also found strong stimulus dependence for gamma synchrony, suggesting that stimulus differences might explain the discrepancy. However, both studies suggest that the attentional enhancement of gamma synchrony in V4 is not attributable to an earlier enhancement in V1 that is passed forward through feedforward projections.

The difference in coherence between superficial and deep layer cells likely has both practical and functional consequences. One practical consequence is that recording studies in the cortex may easily miss much gamma synchrony if the recordings are biased toward the deep layers. In our experience, for example, penetrations through a thickened dura can lead to deep dimpling and eventual punch-through of the electrode to the deep layers. Chronic electrode arrays with fixed 1-mm electrode lengths (50) may also be biased toward the deep layers, depending on the thickness of the cortex, and may consequently find relatively less gamma coherence. It will be important to localize precisely which layers exhibit different forms of synchrony in future studies, preferably using translaminar electrodes that can sample all layers simultaneously (46).

A major functional consequence of laminar differences in synchrony is that gamma- and alpha-band synchrony will be communicated preferentially to different anatomical targets of a given cortical area. The deep layers are the major source of subcortical projections: Layer 5 cells project to the superior colliculus and basal ganglia, and layer 6 cells project to the thalamus (51, 52). The deep layers are also a major source of corticocortical feedback connections, and the ratio of deep to superficial cells making feedback connections increases with distance in the cortical hierarchy (53–55) Almost the exact opposite is found for feedforward connections, which predominantly arise from layers 2/3, especially for long-range connections (55). Thus, gamma-band coherence in a given cortical area is most likely to have an effect on downstream areas, whereas low-frequency coherence is most likely to have an effect on upstream areas and subcortical structures.

Methods

Surgical Procedures. Experiments were performed in areas V1, V2, and V4 in four hemispheres of two male rhesus monkeys (*Macaca mulatta*). All procedures followed the guidelines of the National Institutes of Health.

Two adult male rhesus monkeys were surgically implanted with a head post, a scleral eye coil, and recording chambers. Surgery was conducted under aseptic conditions with isoflurane anesthesia, and antibiotics and analgesics were administered postoperatively. Preoperative MRI was used to identify the stereotaxic coordinates of V1, V2, and V4. V4 recording chambers were placed over the prelunate gyrus. Additional plastic recording chambers were used for V1 and V2 recordings, centered 15 mm lateral and 15 mm dorsal to the occipital crest. The skull remained intact during the initial surgical procedure, and small holes (~3 mm in diameter) were later drilled within the recording chambers under ketamine anesthesia and xylazine analgesic to expose the dura for electrode penetrations.

Behavioral Task. While the monkey fixated a central spot, two stimuli were presented at equal eccentricity, one inside and one outside the recorded neurons' receptive fields (RFs) (Fig. 1*A*). On alternating blocks of trials, the monkey attended to the stimulus either inside or outside the recorded neurons' RF. The monkey was rewarded for releasing a bar when it detected a subtle color change in the attended stimulus while ignoring any change in the unattended stimulus. The color change could occur at any time between 500 and 5,000 ms after stimulus onset, thus requiring the monkey to sustain attention for a long period. Neuronal responses were compared during trials when attention was directed to the stimulus located inside (attention IN) vs. outside (attention OUT) the RF. The hit rate for successful target color change detection was 92.3%, and the false alarm rate for bar releases to the

distracter color change was 4.2%. The sensory conditions were identical across attention conditions.

Recording Techniques. In each recording session, four to eight tungsten microelectrodes (impedances of 1–2 MΩ) were advanced at a very slow rate (1.5 μm/s) to minimize deformation of the cortical surface by the electrode ("dimpling"). For V1 and V4 recordings, we lowered the electrodes slowly until we observed neuronal activity for which we could map an RF. In some of the recordings, we left half of the electrodes (n = 2–4) at that location (supragranular layers) and moved the other half of the electrodes another 1–1.5 mm into the cortex (infragranular layers). We allowed the electrodes to settle for about 30 min and then adjusted each of the electrodes independently as needed to increase the neuronal signal. We then remapped the RFs and began the recording experiment. The V2 recordings were located in the posterior bank of the lunate sulcus. Accordingly, we moved the electrodes through area V1 to reach area V2. For area V2, we used the same recording procedure as in V1 and V4, except that the first V2 neurons encountered were in the infragranular layers.

Electrode tips were separated laterally by 650 or 900 μm. Data amplification, filtering, and acquisition were performed with a Multichannel Acquisition Processor (Plexon). The signal from each electrode was passed through a head stage with unit gain. The signals were filtered from 250 Hz to 8 kHz, further amplified, and digitized at 40 kHz. A threshold was set interactively, and spike waveforms were stored for a time window from 150 μs before to 700 μs after threshold crossing. The threshold clearly separated spikes from noise but was chosen to include multiunit activity. Offline, we performed a principal component analysis of the waveforms and plotted the first principal component against the second principal component. Those waveforms that corresponded to artifacts were excluded. Spikes were sorted into single units. When this was not possible, multiunits were accepted. The times of threshold crossing were kept and downsampled to 1 kHz. RF position and neuronal stimulus selectivity were as expected for the target part of each visual area. For LFP recordings, the signals were filtered with a passband of 0.7–170 Hz, further amplified, and digitized at 1 kHz.

Visual Stimulation and Experimental Paradigm. Stimuli were presented on a 17-in cathode ray tube monitor 0.57 m from the monkey's eyes that had a resolution of 800 × 600 pixels and a screen refresh rate of 120 Hz noninterlaced. Stimulus generation and behavioral control were accomplished with the CORTEX software package. A trial began when the monkey touched a bar and directed its gaze within 0.7° of the fixation cross on the computer screen (Fig. 1*A*). After achieving fixation for 300 ms (1,000 ms for some of the recordings), the stimuli were presented. The stimuli consisted of two circular patches of drifting square-wave luminance grating (100% contrast, diameter of 2°–3°, drift rate of 1°–2°/s, 1–2 cycles/degree of spatial frequency). One stimulus was positioned inside the recorded neurons' RF, and the other was positioned at an equal eccentricity in an adjacent visual field quadrant. The task of the monkey was to release the bar between 150 and 650 ms after a change in stimulus color (i.e., a change of the white stripes of the grating to photometrically isoluminant yellow). That change in stimulus color occurred at an unpredictable moment in time between 500 and 5,000 ms after stimulus onset. All times during this period were equally likely for the color change. Successful trial completion was rewarded with four drops of diluted apple juice. If the monkey released the bar too early or if it moved its gaze out of the fixation window, the trial was immediately aborted and followed by a timeout.

Recordings and Depth Classification. Small clusters of cells (multiunits, termed cells for convenience) and LFPs were recorded on two to four nearby electrodes in each recording session. Cells on different electrodes always had overlapping RFs. We separated recording sites into superficial vs. deep based on depth in the cortex. Along the electrode trajectories, cortical thickness was at least 1.5 mm and was often 2 mm or more, depending on the angle of the electrode penetration to the cortex. We considered recording sites to be in the superficial layers if they were the first responsive cells recorded near the surface, with a maximum distance of 1 mm from the cortical surface. We included in this study all the cells recorded in a previous study of V4 (3), which we classified as "superficial" because of the strong bias to record from the first active cells. We considered recording sites to be in the deep layers if they were recorded more than 1 mm deeper than the first superficial layers cells. For some deep sites, we also advanced the electrodes to the white matter to verify that the deep sites were within 0.5–1 mm of the white matter. Although crudely classifying sites as superficial vs. deep based on electrode depths such as this almost certainly resulted in the misclassification of some sites near the middle layers, any misclassification should only have reduced differences in neuronal properties between the layers rather than create illusory differences that were not actually present in the cortex.

Data Analysis. All analyses were performed using custom programming in Matlab (Mathworks) and using FieldTrip, an open source Matlab toolbox. We quantified power and coherence spectra separately for the prestimulus period and for the sustained epoch with constant visual stimulation until the first stimulus change (excluding the first 300 ms after stimulus onset with response onset transients). For both time epochs, we cut the data into nonoverlapping time segments (300 ms, spectral resolution of 3.33 Hz) and equated the signals for possible firing rate differences across attention conditions. To eliminate any possible contribution of firing rate differences across conditions to coherence values, we equated firing rates across attention conditions using procedures described previously (21). Coherence spectra were calculated between the spiking activity obtained on one electrode and the spiking activity or the LFP activity derived from a different electrode positioned in the same cortical layer. For each comparison between conditions, we equalized the number of data segments for both conditions before spectral analysis by randomly discarding data epochs from the condition with a higher number of segments. This equalization prevents any bias for the spectral estimates that could potentially be introduced by unequal numbers of trials.

Exploratory data analysis demonstrated oscillatory components at low (~10–15 Hz) and high (~60 Hz) frequencies, which occupied frequency bands that varied in width, with the width increasing with the main frequency of the component. For this reason, we used different tapers for the analysis of low and high frequencies. For frequencies up to 22 Hz, we used a single Hanning taper and applied fast-Fourier transforms to the Hanning-tapered trials. For frequencies beyond 22 Hz, we used multitaper methods to achieve optimal spectral concentration (2, 56–58). For frequencies between 20 and 100 Hz, we used five Slepian tapers, providing an effective taper smoothing of ±10 Hz.

ACKNOWLEDGMENTS. We thank D. Heister and P. Su for their help with data collection. This study was supported by National Eye Institute Grants EY017292 and EY017921 (to R.D.).

1. Fries P, Reynolds JH, Rorie AE, Desimone R (2001) Modulation of oscillatory neuronal synchronization by selective visual attention. *Science* 291:1560–1563.
2. Womelsdorf T, Fries P, Mitra PP, Desimone R (2006) Gamma-band synchronization in visual cortex predicts speed of change detection. *Nature* 439:733–736.
3. Fries P, Womelsdorf T, Oostenveld R, Desimone R (2008) The effects of visual stimulation and selective visual attention on rhythmic neuronal synchronization in macaque area V4. *J Neurosci* 28:4823–4835.
4. Taylor K, Mandon S, Freiwald WA, Kreiter AK (2005) Coherent oscillatory activity in monkey area v4 predicts successful allocation of attention. *Cereb Cortex* 15:1424–1437.
5. Bichot NP, Rossi AF, Desimone R (2005) Parallel and serial neural mechanisms for visual search in macaque area V4. *Science* 308:529–534.
6. Desimone R, Duncan J (1995) Neural mechanisms of selective visual attention. *Annu Rev Neurosci* 18:193–222.
7. Hayden BY, Gallant JL (2005) Time course of attention reveals different mechanisms for spatial and feature-based attention in area V4. *Neuron* 47:637–643.
8. Maunsell JH, McAdams CJ (2001) Effects of attention on the responsiveness and selectivity of individual neurons in visual cerebral cortex. *Visual Attention and Cortical Circuits*, eds Braun J, Koch C, Davis JL (MIT Press, Cambridge, MA), pp 103–119.
9. Moran J, Desimone R (1985) Selective attention gates visual processing in the extrastriate cortex. *Science* 229:782–784.
10. Reynolds JH, Pasternak T, Desimone R (2000) Attention increases sensitivity of V4 neurons. *Neuron* 26:703–714.
11. Treue S (2001) Neural correlates of attention in primate visual cortex. *Trends Neurosci* 24:295–300.
12. Mitchell JF, Sundberg KA, Reynolds JH (2007) Differential attention-dependent response modulation across cell classes in macaque visual area V4. *Neuron* 55: 131–141.
13. Cohen MR, Maunsell JH (2009) Attention improves performance primarily by reducing interneuronal correlations. *Nat Neurosci* 12:1594–1600.
14. Mitchell JF, Sundberg KA, Reynolds JH (2009) Spatial attention decorrelates intrinsic activity fluctuations in macaque area V4. *Neuron* 63:879–888.
15. Niebur E, Koch C, Rosin C (1993) An oscillation-based model for the neuronal basis of attention. *Vision Res* 33:2789–2802.
16. Salinas E, Sejnowski TJ (2001) Correlated neuronal activity and the flow of neural information. *Nat Rev Neurosci* 2:539–550.
17. Börgers C, Kopell NJ (2008) Gamma oscillations and stimulus selection. *Neural Comput* 20:383–414.

18. Buschman TJ, Miller EK (2007) Top-down versus bottom-up control of attention in the prefrontal and posterior parietal cortices. *Science* 315:1860–1862.
19. Armstrong KM, Fitzgerald JK, Moore T (2006) Changes in visual receptive fields with microstimulation of frontal cortex. *Neuron* 50:791–798.
20. Saalmann YB, Pigarev IN, Vidyasagar TR (2007) Neural mechanisms of visual attention: How top-down feedback highlights relevant locations. *Science* 316:1612–1615.
21. Gregoriou GG, Gotts SJ, Zhou H, Desimone R (2009) High-frequency, long-range coupling between prefrontal and visual cortex during attention. *Science* 324: 1207–1210.
22. Buffalo EA, Fries P, Landman R, Liang H, Desimone R (2010) A backward progression of attentional effects in the ventral stream. *Proc Natl Acad Sci USA* 107:361–365.
23. Grossberg S (2007) Consciousness CLEARS the mind. *Neural Netw* 20:1040–1053.
24. Silva LR, Amitai Y, Connors BW (1991) Intrinsic oscillations of neocortex generated by layer 5 pyramidal neurons. *Science* 251:432–435.
25. Flint AC, Connors BW (1996) Two types of network oscillations in neocortex mediated by distinct glutamate receptor subtypes and neuronal populations. *J Neurophysiol* 75: 951–957.
26. Sun W, Dan Y (2009) Layer-specific network oscillation and spatiotemporal receptive field in the visual cortex. *Proc Natl Acad Sci USA* 106:17986–17991.
27. Lopes Da Silva FH, Storm Van Leeuwen W (1977) The cortical source of the alpha rhythm. *Neurosci Lett* 6:237–241.
28. Bollimunta A, Chen Y, Schroeder CE, Ding M (2008) Neuronal mechanisms of cortical alpha oscillations in awake-behaving macaques. *J Neurosci* 28:9976–9988.
29. Jones SR, Pinto DJ, Kaper TJ, Kopell N (2000) Alpha-frequency rhythms desynchronize over long cortical distances: A modeling study. *J Comput Neurosci* 9:271–291.
30. Lorincz ML, Kékesi KA, Juhász G, Crunelli V, Hughes SW (2009) Temporal framing of thalamic relay-mode firing by phasic inhibition during the alpha rhythm. *Neuron* 63: 683–696.
31. Roopun AK, et al. (2006) A beta2-frequency (20-30 Hz) oscillation in nonsynaptic networks of somatosensory cortex. *Proc Natl Acad Sci USA* 103:15646–15650.
32. Gray CM, McCormick DA (1996) Chattering cells: Superficial pyramidal neurons contributing to the generation of synchronous oscillations in the visual cortex. *Science* 274:109–113.
33. Nowak LG, Azouz R, Sanchez-Vives MV, Gray CM, McCormick DA (2003) Electrophysiological classes of cat primary visual cortical neurons in vivo as revealed by quantitative analyses. *J Neurophysiol* 89:1541–1566.
34. Maier A, Adams GK, Aura C, Leopold DA (2010) Distinct superficial and deep laminar domains of activity in the visual cortex during rest and stimulation. *Front Syst Neurosci* 4. pii. 31.
35. von Stein A, Chiang C, König P (2000) Top-down processing mediated by interareal synchronization. *Proc Natl Acad Sci USA* 97:14748–14753.
36. Ray WJ, Cole HW (1985) EEG alpha activity reflects attentional demands, and beta activity reflects emotional and cognitive processes. *Science* 228:750–752.
37. Klimesch W, Doppelmayr M, Russegger H, Pachinger T, Schwaiger J (1998) Induced alpha band power changes in the human EEG and attention. *Neurosci Lett* 244:73–76.
38. Worden MS, Foxe JJ, Wang N, Simpson GV (2000) Anticipatory biasing of visuospatial attention indexed by retinotopically specific alpha-band electroencephalography increases over occipital cortex. *J Neurosci*, 20:RC63 (1–6).
39. Thut G, Nietzel A, Brandt SA, Pascual-Leone A (2006) Alpha-band electroencephalographic activity over occipital cortex indexes visuospatial attention bias and predicts visual target detection. *J Neurosci* 26:9494–9502.
40. Ergenoglu T, et al. (2004) Alpha rhythm of the EEG modulates visual detection performance in humans. *Brain Res Cogn Brain Res* 20:376–383.
41. Hanslmayr S, et al. (2007) Prestimulus oscillations predict visual perception performance between and within subjects. *Neuroimage* 37:1465–1473.
42. van Dijk H, Schoffelen JM, Oostenveld R, Jensen O (2008) Prestimulus oscillatory activity in the alpha band predicts visual discrimination ability. *J Neurosci* 28: 1816–1823.
43. Kelly SP, Lalor EC, Reilly RB, Foxe JJ (2006) Increases in alpha oscillatory power reflect an active retinotopic mechanism for distracter suppression during sustained visuospatial attention. *J Neurophysiol* 95:3844–3851.
44. Rihs TA, Michel CM, Thut G (2007) Mechanisms of selective inhibition in visual spatial attention are indexed by alpha-band EEG synchronization. *Eur J Neurosci* 25:603–610.
45. Yamagishi N, et al. (2003) Attentional modulation of oscillatory activity in human visual cortex. *Neuroimage* 20:98–113.
46. Lakatos P, et al. (2009) The leading sense: Supramodal control of neurophysiological context by attention. *Neuron* 64:419–430.
47. Schroeder CE, Lakatos P (2009) Low-frequency neuronal oscillations as instruments of sensory selection. *Trends Neurosci* 32:9–18.
48. Poort J, Roelfsema PR (2009) Noise correlations have little influence on the coding of selective attention in area V1. *Cereb Cortex* 19:543–553.
49. Chalk M, et al. (2010) Attention reduces stimulus-driven gamma frequency oscillations and spike field coherence in V1. *Neuron* 66:114–125.
50. Kelly RC, et al. (2007) Comparison of recordings from microelectrode arrays and single electrodes in the visual cortex. *J Neurosci* 27:261–264.
51. Salin PA, Bullier J (1995) Corticocortical connections in the visual system: Structure and function. *Physiol Rev* 75:107–154.
52. Felleman DJ, Van Essen DC (1991) Distributed hierarchical processing in the primate cerebral cortex. *Cereb Cortex* 1:1–47.
53. Rockland KS, Van Hoesen GW (1994) Direct temporal-occipital feedback connections to striate cortex (V1) in the macaque monkey. *Cereb Cortex* 4:300–313.
54. Kennedy H, Bullier J (1985) A double-labeling investigation of the afferent connectivity to cortical areas V1 and V2 of the macaque monkey. *J Neurosci* 5: 2815–2830.
55. Barone P, Batardiere A, Knoblauch K, Kennedy H (2000) Laminar distribution of neurons in extrastriate areas projecting to visual areas V1 and V4 correlates with the hierarchical rank and indicates the operation of a distance rule. *J Neurosci* 20: 3263–3281.
56. Jarvis MR, Mitra PP (2001) Sampling properties of the spectrum and coherency of sequences of action potentials. *Neural Comput* 13:717–749.
57. Mitra PP, Pesaran B (1999) Analysis of dynamic brain imaging data. *Biophys J* 76: 691–708.
58. Pesaran B, Pezaris JS, Sahani M, Mitra PP, Andersen RA (2002) Temporal structure in neuronal activity during working memory in macaque parietal cortex. *Nat Neurosci* 5: 805–811.

Supporting Information

Buffalo et al. 10.1073/pnas.1011284108

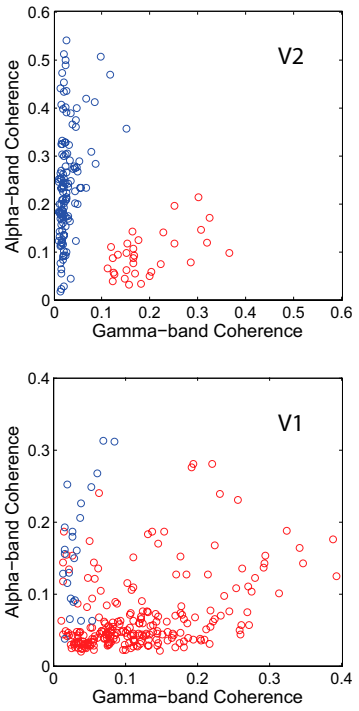

Fig. S1. Distribution of coherence in gamma- and alpha-bands for superficial and deep recordings across areas. Across areas V2 (*Upper*) and V1 (*Lower*), superficial layer recordings (red) demonstrated stronger gamma-band coherence, whereas deep layer recordings (blue) demonstrated stronger alpha-band coherence.

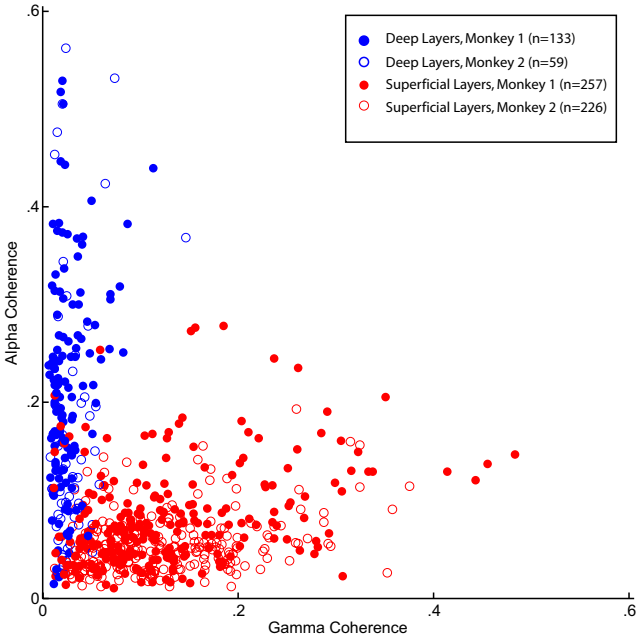

Fig. S2. Distribution of coherence in gamma- and alpha-bands for superficial and deep recordings across all three areas, separated by monkey. Across all three areas, a similar pattern of results was observed in both monkeys (open and filled circles). Superficial recordings (red) demonstrated primarily gamma-band coherence, and deep recordings (blue) demonstrated primarily alpha-band coherence.

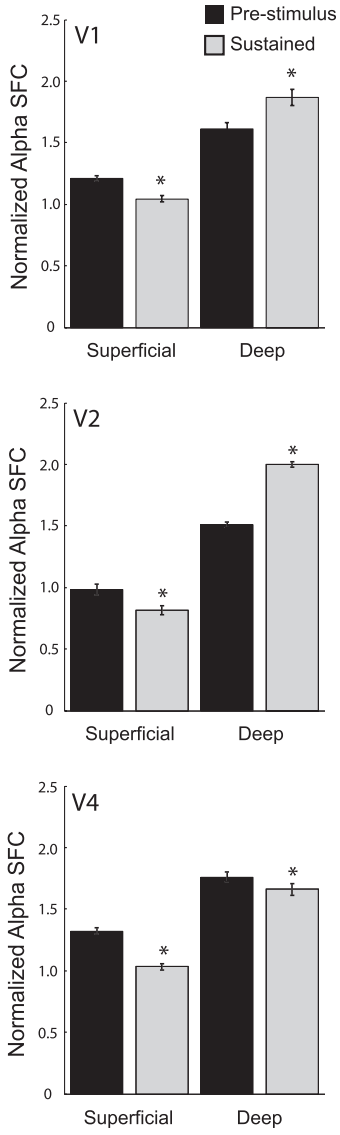

Fig. S3. Comparison between pre- and poststimulation alpha-band coherence. The magnitude of alpha-band coherence as a function of stimulation period is shown for superficial and deep layer recordings across areas V1 (*Top*), V2 (*Middle*), and V4 (*Bottom*). Black bars represent the prestimulus period, and gray bars represent the period from 300 ms after stimulus onset until the first stimulus change. *$P < 0.05$, comparison between pre- and poststimulus periods.

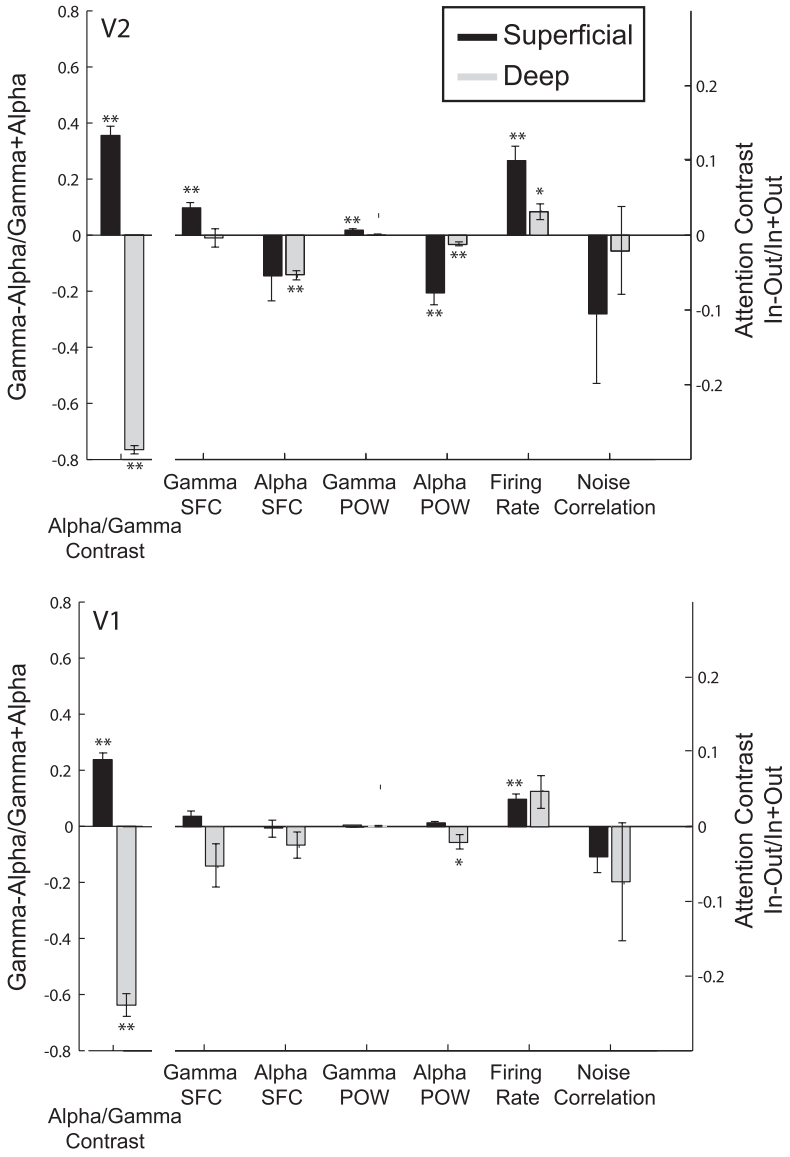

Fig. S4. Attentional effects across areas for superficial and deep layer recordings. Contrast indices (In − Out/In + Out) of the effects of attention were calculated for several measures across areas V2 (*Upper*) and V1 (*Lower*). Superficial recordings are shown in black, and deep recordings are shown in gray. *$P < 0.05$; **$P < 0.01$. All comparisons are sign tests, relative to zero.

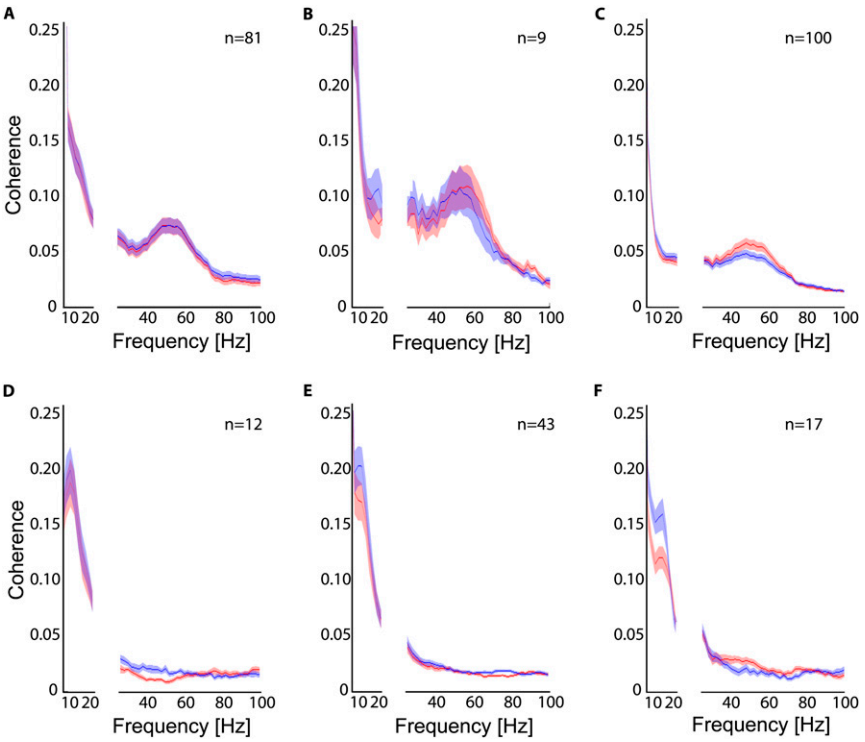

Fig. S5. Attentional modulation of SSC in areas V1, V2, and V4. Red traces represent SSC in each area, with attention directed INTO the neuron's RF. Blue traces represent SSC with attention directed OUT of the RF. The magnitude of coherence as a function of frequency is shown for superficial recordings (*A*–*C*) and deep recordings (*D*–*F*) for areas V1 (*A* and *D*), V2 (*B* and *E*), and V4 (*C* and *F*). Shaded areas represent SEM.